Synthesis and Characterization of Ultrafine Tungsten and Tungsten Oxide Nanoparticles by a Reverse Microemulsion-Mediated Method

Liufeng Xiong and Ting He*

Honda Research Institute USA, Incorporated, 1381 Kinnear Road, Columbus, Ohio 43212

Received October 21, 2005. Revised Manuscript Received March 6, 2006

Ultrafine tungsten and tungsten oxide powders with controllable particle size and structure have been synthesized by a reverse microemulsion-mediated synthesis method. The nanoparticles were characterized by transmission electron microcopy, X-ray diffraction, and thermal analysis. Synthesis conditions, including water-to-surfactant ratio, annealing temperature, water-to-alkoxide ratio, and drying method, have been shown to be critical in controlling the size and structure of tungsten nanoparticles. Using the same synthesis technique, carbon-supported metallic tungsten and tungsten oxide nanoparticles with controllable size and dispersion can also be prepared. The ultrafine nanoparticles prepared by this synthesis method may find interesting applications in various fields such as catalysis, electronics, illumination, gas sensors, and so forth.

Introduction

Nanosized materials have attracted great attention as a result of displaying unique size-dependent features. Tungsten based materials, including metallic tungsten and tungsten oxide, offer very interesting physical and chemical properties. For example, metallic tungsten has a high melting point (3410 °C), exhibits high-temperature strength and thermal stability, and has high thermal and electrical conductivities. Metallic tungsten has been widely applied as a thermionic cathode material,[1,2] in field electronics,[3,4] as an electrical contact material,[5] and as a raw material for ultrahard alloys in high-speed steels, cutting tools, and anti-friction tools.[6] In parallel, tungsten oxide offers special electrochromic,[7] catalytic,[8] and gas sensing properties.[9] However, preparation of tungsten and tungsten oxide nanoparticles down to a few nanometers has been a challenge.

Common methods to prepare metallic tungsten include high-temperature (>1000° C) reduction of WO_3 with H_2, carbon, or calcium; high-temperature reduction of WF_6 with hydrogen;[6] and self-propagating high-temperature synthesis.[10] These high-temperature methods usually fail to produce nanosized tungsten particles. Low-temperature synthesis methods, such as chemical reduction[11] and reaction of tungsten complexes with organopolysilane oligomers,[12] often show amorphous structures with particle sizes larger than 15 nm. In addition, chemical reduction methods normally employ strong reducing agents (e.g., trialkylborohydride) that result in reactant contamination.[11] X-ray photoelectron spectroscopy reveals that chemically reduced tungsten is hexavalent instead of metallic,[13] indicating the particles are partially or completely oxidized. Similarly, tungsten particles synthesized by the reaction of tungsten complexes with organopolysilane oligomers show oxidized shells.[10] Further synthesis methods include laser assisted chemical vapor deposition,[14,15] thermal decomposition of tungsten hexacarbonyl,[3] and electron-beam-induced selective deposition.[16] However, none of these synthesis methods have fabricated tungsten nanoparticles down to a few nanometers with uniform size distribution.

Tungsten oxide powders and films have been prepared by various methods, including chemical vapor deposition,[17,18] magnetron sputtering,[19] cathodic arc deposition,[20] laser vaporization,[21,22] electrochemical deposition,[23] wet chemical deposition,[24] sol−gel process,[25−29] hydrothermal reac-

* To whom correspondence should be addressed. E-mail: the@honda-ri.com.

(1) Wang, F.-Z.; Zhang, H.; Ding, B.-J.; Zhu, R.-H. *Mater. Sci. Eng., A* **2002**, *336*, 59.
(2) Selcuka, C.; Benthamb, R.; Morleyb, N.; Woodc, J. V. *Mater. Lett.* **2004**, *58*, 1873.
(3) Magnusson, M. H.; Deppert, K. *J. Mater. Res.* **2000**, *15*, 1564.
(4) Schmitz, J. E. J. *Chemical vapor deposition of tungsten and tungsten silicides for VLSI/ULSI applications*; Noyes: Park Ridge, NJ, U.S.A., 1992.
(5) Kang, H. *J. Nucl. Mater.* **2004**, *335*, 1.
(6) Bailar, J. C.; Emeleus, H. J. *Comput. Inorg. Chem.* **1973**, *3*, 742.
(7) Franke, E. B.; Trimble, C. L.; Hale, J. S.; Schubert, M.; Woolam, J. A. *J. Appl. Phys.* **2000**, *88*, 5777.
(8) Engweiler, J.; Harf, J.; Baiker, A. *J. Catal.* **1996**, *159*, 259.
(9) Lee, D. S.; Nam, K. H.; Lee, D. D. *Thin Solid Films* **2000**, *375*, 142.
(10) Won, C.-W.; Jung, J.-C.; Ko, S.-G.; Lee, J.-H. *Mater. Res. Bull.* **1999**, *34*, 2239.
(11) Zeng, D.; Hampden-Smith, M. J. *Chem. Mater.* **1993**, *5*, 681.
(12) Chang, Y.; Wang, H.; Chiu, C.; Cheng, D.; Yen, M.; Chiu, H. *Chem. Mater.* **2002**, *14*, 4334.
(13) Goetz, M.; Wendt, H. *J. Appl. Electrochem.* **2001**, *31*, 811.
(14) Landstrom, L.; Kokavecz, J.; Lu, J.; Heszler, P. *J. Appl. Phys.* **2004**, *95*, 4408.
(15) Landstrom, L.; Lu, J.; Heszler, P. *J. Phys. Chem. B* **2003**, *107*, 11615.
(16) Xie, G.; Song, M.; Mitsuishi, K.; Furuya, K. *J. Vac. Sci. Technol., B* **2004**, *22*, 2589.
(17) Brescacin, E.; Basato, M.; Tondello, E. *Chem. Mater.* **1999**, *11*, 314.
(18) Davazoglou, D.; Moutsakis, A.; Valamontes, V.; Psycharis, V.; Tsamakis, D. *J. Electrochem. Soc.* **1997**, *144*, 595.
(19) Okeefe, M. J.; Grant, J. T.; Solomon, J. S. *J. Electron. Mater.* **1995**, *24*, 961.
(20) Anders, S.; Anders, A.; Rubin, M.; Wang, Z.; Raoux, S.; Kong, F.; Brown, I. G. *Surf. Coat. Technol.* **1995**, *76*, 167−173.
(21) Sun, M.; Xu, N.; Cao, J. W.; Yao, J. N.; Wang, E. C. *J. Mater. Res.* **2000**, *15*, 927.
(22) Li, S. T.; El-Shall, M. S. *Nanostruct. Mater.* **1999**, *12*, 215.
(23) Yu, Z.; Jia, X.; Du, J.; Zhang, J. *Sol. Energy Mater. Sol. Cells* **2000**, *64*, 55.

10.1021/cm052320t CCC: $33.50
Published on Web 03/30/2006

tions,[30,31] and ultrasound irradiation of tungsten hexacarbonyl in diphenylmethane.[32] Organic ligand and emulsion based methods have also been employed to prepare tungsten oxides;[33] however, high-temperature calcinations (>500 ° C) are needed to remove surfactants resulting in a reduction of surface area and an increase in particle size. Despite the numerous methods reported for the preparation of tungsten oxide powders, synthesis of powders with particle sizes less than 5 nm, to the best of our knowledge, has yet to be reported.

In recent years, reverse microemulsion methods have been explored to synthesize metals, ceramics, and polymers.[34−36] Particles with well-defined geometry and size can be obtained by this synthesis approach because all processes are confined in nanosized water droplets (nanoreactors). Reported here, to the best of our knowledge, is the first demonstration of synthesizing tungsten metal and tungsten oxide powders with particle sizes less than 5 nm using a reverse microemulsion-mediated synthesis method.

Experimental Section

Chemicals. An ionic surfactant (AOT, sodium bis(2-ethylhexyl)-sulfosuccinate; Acros Organics) and two nonionic surfactants (Brij-30, polyoxyethylene (4) lauryl ether; Triton X-100, polyoxyethylene (10) octylphenyl ether; Acros Organics) were utilized as received. 2-Hexanol (99%; Acros Organics) was used as the cosurfactant with Triton X-100. Cyclohexane and *n*-heptane (99%; Acros Organic) were used as continuous nonpolar liquids (oil phases) for the reverse microemulsions. Tungsten isopropoxide (50 mg/mL in 2-propanol; Chemat Technology) was used as the tungsten alkoxide precursor.

Synthesis. Figure 1 schematically illustrates the general procedure for using a reverse microemulsion synthesis technique to fabricate metallic tungsten and tungsten oxide nanoparticles. The synthesis involves (i) preparing a reverse microemulsion and tungsten alkoxide solution; (ii) hydrolyzing the tungsten alkoxide in the reverse microemulsion; (iii) aging the reaction products; (iv) collecting and drying the particles; and (v) heat treating at appropriate temperatures under controlled gas atmospheres.

Preparation of Reverse Microemulsion. Reverse microemulsions were prepared by adding surfactant to a water/oil mixture, ultrasonically blending for 15 min, and stirring at room temperature until a clear, stable emulsion was obtained. Two microemulsion systems were prepared for the nano-synthesis: Brij-30/*n*-heptane and Triton X-100/*n*-hexanol/cyclohexane. The Brij-30/*n*-heptane microemulsion system consisted of 13% Brij-30 and 87% *n*-heptane, and the Triton X-100/*n*-hexanol/cyclohexane microemulsion system consisted of 5.4% Triton X-100, 4.7% *n*-hexanol, and 89.9% cyclohexane (volume ratio). The water-to-surfactant ratio (ω) in these microemulsion systems varied from 3 to 10.

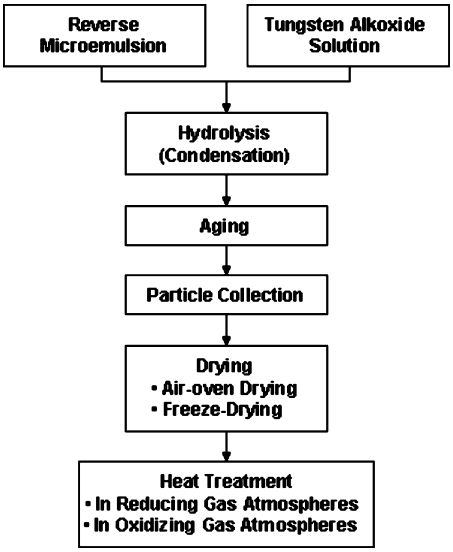

Figure 1. Schematic illustration of the synthesis processes to fabricate tungsten oxide and metallic tungsten nanoparticles.

Hydrolysis of Tungsten Alkoxide. Tungsten alkoxide was dispersed in pre-degassed cyclohexane or heptane. No sign of hydrolysis was observed indicating that the water content in the solvent and precursor was negligible. The tungsten alkoxide solution was then slowly added to the microemulsion under continuous stirring. The water to alkoxide molar ratios varied between 3 and 20. The hydrolysis reaction occurred slowly at room temperature, as reflected by a slow increase of solution opacity. The mixture was aged at room temperature for 4−96 h under continuous stirring.

Particle Collection and Drying. After aging, the particles were recovered from the reverse microemulsion by various techniques. Filtration was not effective in collecting the particles resulting in low yields. Therefore, centrifugation plus air-drying or freeze-drying methods were employed. The typical centrifugation process involved precipitation by adding acetone, discarding the top solution, and centrifuging the remaining mixtures. However, the particles prepared with Triton X-100 did not precipitate, and centrifugation was directly used. The collected particles were then repeatedly washed with acetone and ethanol to remove the surfactant and dried in air at 70 °C or by freeze drying. For freeze drying, the particles were redispersed in deionized water after washing and quickly frozen by liquid nitrogen. The powders were then collected after all the water was removed.

To prepare carbon-supported tungsten oxide or metallic tungsten nanoparticles, high surface area carbon powder (Ketjen Black) was added to the reaction mixtures after completion of the hydrolysis reaction. The resultant was ultrasonically blended for 15 min and stirred for 1 h. The particles were then precipitated by adding acetone, washed with acetone and ethanol, collected by centrifugation, and dried by blowing with Ar.

Heat Treatment. After drying, the collected powders were heat treated at appropriate temperatures under defined gas atmospheres. Tungsten oxide nanoparticles were prepared by heat treating the hydrolysis products at temperatures ranging from 200 to 500 °C for 2 h under flowing air with a heating rate of 5 °C/min. Metallic tungsten nanoparticles were obtained by reducing the tungsten hydrolysis products in reducing gas atmospheres. Typically, the tungsten containing nanoparticles were first heated to 300 °C in

(24) Krings, L. H. M.; Talen, W. *Sol. Energy Mater. Sol. Cells* **1998**, *54*, 27.
(25) Cheng, W.; Baudrin, E.; Dunn, B.; Zink, J. L. *J. Mater. Chem.* **2001**, *11*, 92.
(26) Munro, B.; Kramer, S.; Zapp, P.; Krug, H. *J. Sol.-Gel Sci. Technol.* **1998**, *13*, 673.
(27) Tamou, Y.; Tanaka, S. *Nanostruct. Mater.* **1999**, *12*, 123.
(28) Bulian, C. J.; Dye, R. C.; Son, S. F.; Jorgensen, B. S.; Perry, W. L. U.S. Patent 2005025700, 2005.
(29) Nogueira, H. I. S.; Cavaleiro, A. M. V.; Rocha, J.; Trindade, T.; Jesus, J. D. P. D. *Mater. Res. Bull.* **2004**, *39*, 683.
(30) Guo, J. D.; Li, Y. J. J.; Whittingham, M. S. *J. Power Sources* **1995**, *54*, 461.
(31) Patil, P. S.; Patil, P. R.; Kadam, L. D.; Pawar, S. H. *Bull. Electrochem.* **1999**, *15*, 307.
(32) Koltypin, Y.; Nikitenkob, S. I.; Gedanken, A. *J. Mater. Chem.* **2002**, *12*, 1107.
(33) Lu, Z.; Kanan, S. M.; Tripp, C. P. *J. Mater. Chem.* **2002**, *12*, 983.
(34) Roy, S.; Sigmund, W.; Aldinger, F. *J. Mater. Res.* **1999**, *14*, 1524.
(35) Lee, H. S.; Lee, W. C.; Furubayashi, T. *J. Appl. Phys.* **1999**, *85*, 5231.
(36) Kaneda, I.; Sogabe, A.; Nakajima, H. *J. Colloid Interface Sci.* **2004**, *275*, 450.

air for 1 h to remove residual organics followed by a heat treatment under flowing pure H_2 or a mixture of H_2/N_2 (1:5 v/v) at temperatures between 500 and 650 °C. Heating rates of 5 °C/min were utilized. After cooling to room temperature, the powder was purged with a flowing mixture of N_2 and air (5:1 volume ratio) for 30 min to form a passivation layer on the surface. As a result of hydrogen flammability issues, all heat treatments were conducted in a well-ventilated hood. Additionally, the samples were purged with an inert gas at room temperature before and after heat treating in hydrogen containing atmospheres.

Characterization. Several characterization tools were used to determine the phase and the morphology of the nanoparticles.

X-ray Diffraction (XRD). The prepared nanoparticles were characterized by XRD using a Bruker powder diffractometer (a combination of model D8 Discover and D8 Advance) equipped with a Ge(Li) solid-state detector (Cu Kα radiation). The diffraction patterns were recorded from $2\theta = 25°$ to $2\theta = 90°$ at a scan rate of 0.02° per step and 5 s per point. The average particle sizes were estimated from diffraction peak broadening using Scherrer's equation.

Transmission Electron Microscopy (TEM). The morphology and size of the nanoparticles were examined by high-resolution transmission electron microscopy (HRTEM) and high-angle annular dark field scanning transmission electron microscopy (HAADF-STEM) using a FEI Tecnai TF-20 microscope. Composition of the nanoparticles was analyzed by an energy-dispersive X-ray (EDX) spectroscope attached to the transmission electron microscope. The samples for analysis were prepared by dispersing nanoparticles in methanol and drop-casting onto a carbon coated copper grid followed by dying in air at room temperature.

Thermal Gravity Analysis and Differential Scanning Calorimetry (TGA-DSC). Thermal analyses were performed by using a TA Instrument model SDT 2960 Simultaneous TGA-DSC. The thermal properties of various surfactants and the effectiveness of removing surfactants from nanoparticle surfaces were determined by TGA-DSC. The samples were heated at a rate of 20 °C/min under flowing air. For analyzing liquid surfactants (Brij-30 and Triton X-100), the surfactant was mixed with carbon and air-dried.

Results and Discussion

1. Surfactant Selection. For applications such as catalysis, surfactant removal from nanoparticle surfaces is necessary to minimize blocking of active catalysis sites. Ideally, surfactants used for synthesis should be easily removed by washing or by heat treating in oxidizing atmospheres at low temperatures to minimize particle growth and loss of surface area. For this purpose, various surfactants were thermally analyzed by TGA-DSC.

TGA-DSC analysis showed that Triton X-100 began to lose weight at about 300 °C and decomposed at about 390 °C as evidenced by an exothermal DSC peak. Another exothermal peak occurring at about 650 °C was caused by burning of the carbon support utilized for the convenience of analysis. Brij-30 displayed similar thermal properties except that the decomposition temperature was slightly lower at about 350 °C. Systematic TGA-DSC analyses revealed that the two surfactants were largely removed by washing with acetone and ethanol. Details of the TGA-DSC data are shown in Supporting Information. The small amount of residual surfactant after washing (<10 wt %) was removed successfully by heat treating in air at 300 °C and was confirmed by thermal analysis. TGA-DSC analysis of the ionic surfactant AOT indicated that about 15 wt % of residue remained even after decomposition at 400 °C in air. The difficulty in removing AOT is most likely due to the presence of sodium and sulfur.

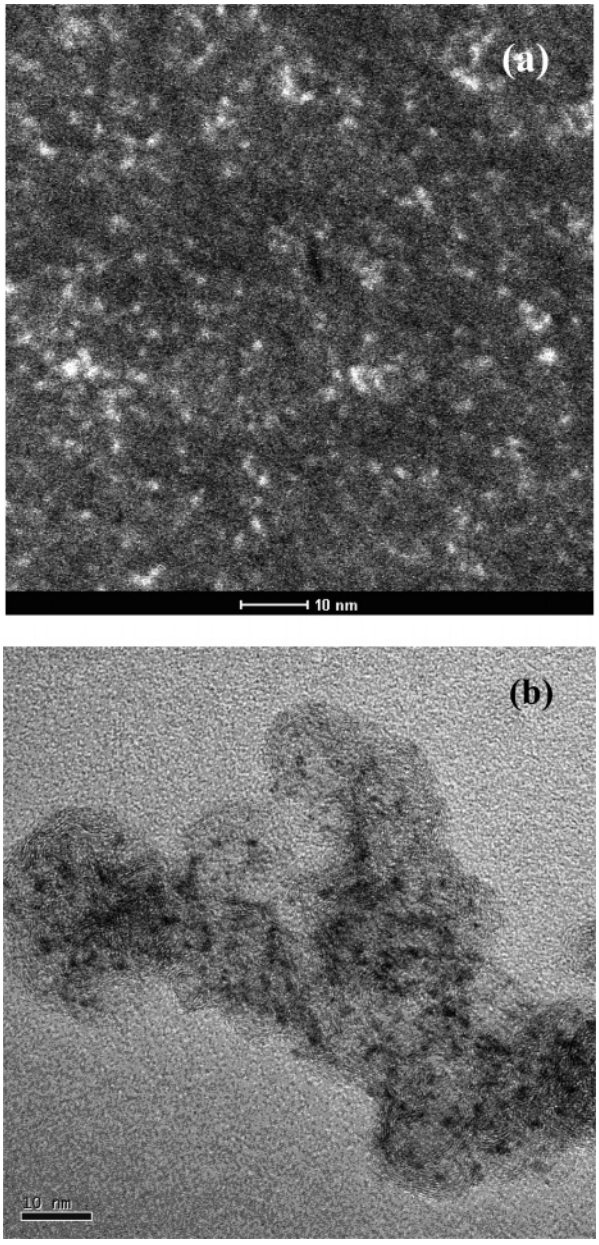

Figure 2. (a) HAADF-STEM micrograph of unsupported tungsten hydrolysis products; (b) HRTEM micrograph of carbon supported tungsten hydrolysis products.

Because ionic surfactants may introduce impurities in the final product and are more difficult to remove from nanoparticle surfaces, nonionic surfactants were used in the synthesis of tungsten nanoparticles. Accordingly, surfactant removal processes involved washing the nanoparticles with acetone and ethanol followed by a 1 h heat treatment at 300 °C in air prior to additional heat treatments to reduce the nanoparticles to metallic tungsten. At this burn-out temperature, as will be shown later, no significant particle growth was observed, in contrast to a case where a much higher burn-out temperature (>500 °C) was required to remove surfactants.[33] The heat treatment at 300 °C in air was not necessary for preparation of tungsten oxide nanoparticles

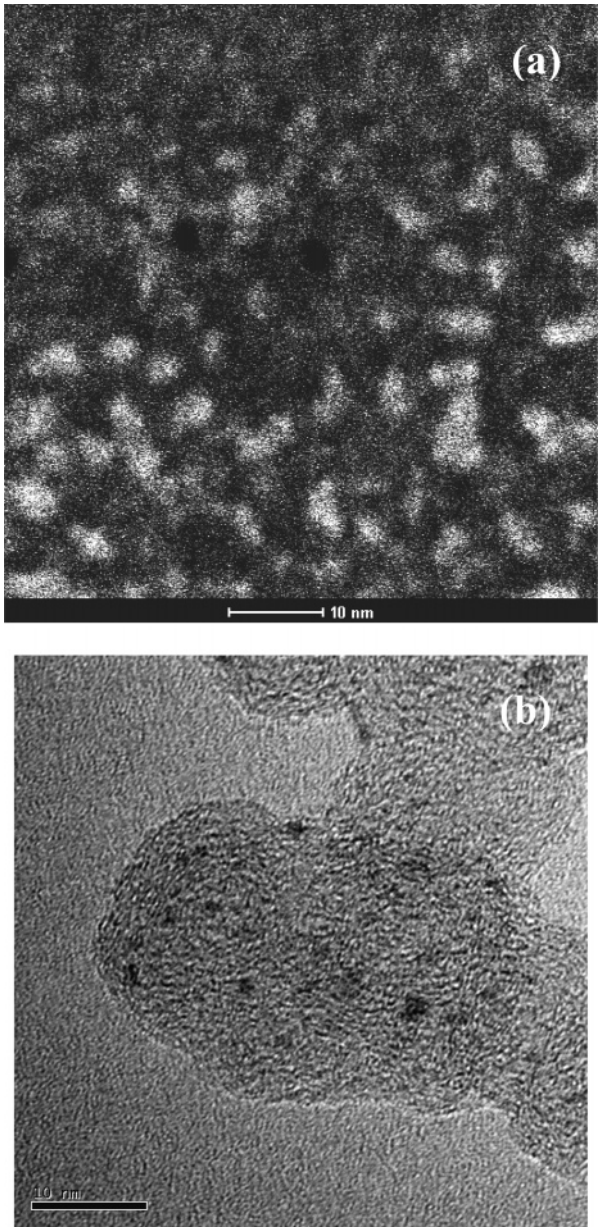

Figure 3. (a) HAADF-STEM micrograph of unsupported tungsten oxides; (b) HRTEM micrograph of carbon supported tungsten oxides. The sample in part a was prepared with a Brij-30/*n*-heptane/water microemulsion, and the sample in b was prepared with a Triton X-100/2-hexanol/cyclohexane/water microemulsion.

because the nanoparticles were heat treated in an oxidizing atmosphere at temperatures usually higher than 300 °C.

2. Synthesis of Tungsten Oxide Nanoparticles. Tungsten oxide nanoparticles may be prepared by the hydrolysis of tungsten alkoxide or through precipitation of sodium tungstate with hydrochloric acid in a reverse microemulsion. After the hydrolysis or precipitation reactions, a heat treatment is necessary to form tungsten oxide. The hydrolysis of tungsten alkoxide does not introduce inorganic impurities from the reactants; it was used in this study.

Figure 2a displays a typical HAADF-STEM micrograph of as-prepared, unsupported tungsten hydrolysis products (i.e, before heat treatment). The HAADF technique, also referred as *Z*-contrast, allows the observation of the interfaces between different elements due to the differences in atomic number, density, or strain field.[37] The bright spots are tungsten

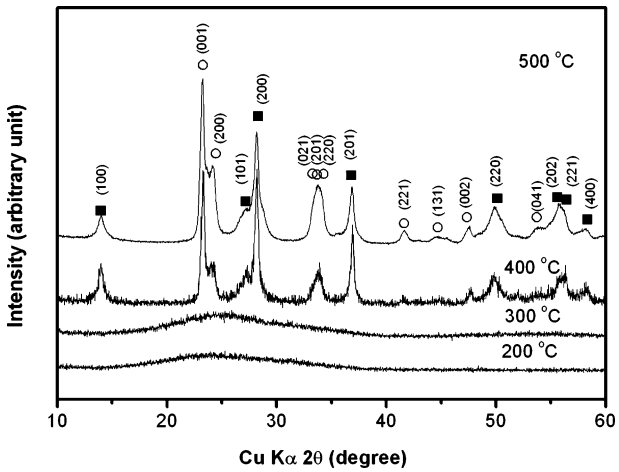

Figure 4. XRD patterns of tungsten oxides heat treated at various temperatures. The samples were prepared with a Brij-30/*n*-heptane/water microemulsion. The symbol ■ refers to WO_3 with hexagonal structure (PDF number 33-1387), and the symbol ○ refers to WO_3 with orthorhombic structure (PDF number 20-1324).

hydrolysis products having a predominantly spherical shape and particle sizes of 1−2 nm. The compositions of particles were further confirmed by EDX analysis which confirmed the presence of tungsten. Increasing the water content (e.g., water-to-surfactant ratio of 10) increased the polydispersity and particle size of the nanoparticles. The size of nanoparticles prepared in reverse microemulsions usually increases with water content because the particle growth is confined in the nanosized water droplet and the size of the water droplet is proportional to the ratio of water to surfactant. However, above a certain water-to-surfactant ratio, the particle size increase is not significant, but the polydispersity increases.[38] Figure 2b displays a typical HRTEM micrograph of carbon supported tungsten hydrolysis products. The darker spots, due to mass contrast, are tungsten containing nanoparticles. The nanoparticles are uniformly dispersed on the carbon support and exhibit predominantly spherical shape with particle sizes ranging from 1 to 2 nm. At higher magnification, no lattice fringes were observed indicating amorphous structure of the tungsten hydrolysis products.

Figure 3a shows a representative HAADF-STEM micrograph of the hydrolysis products after heat treating at 500 °C in air. The bright spots are tungsten oxide nanoparticles that are predominantly spherical and have particle sizes ranging from 2 to 4 nm. The HRTEM image of carbon supported tungsten oxides is shown in Figure 3b where the tungsten oxide nanoparticles (darker spots) are uniformly dispersed on the carbon surface with particle sizes ranging from 2 to 3 nm. The size similarity between supported and unsupported tungsten oxide particles indicates that the synthesis of tungsten oxide is not strongly dependent on support materials, whereas the size of particles produced using the conventional impregnation method depends largely on the surface area and surface functionality of the supporting material.[39,40] The results imply the possibility of using other

(37) Garcia-Gutierrez, D.; Gutierrez-wing, C.; Miki-Yoshida, M.; Jose-Yacaman, M. *Appl. Phys. A* **2004**, *79*, 481.
(38) Pileni, M. P. *Langmuir* **1997**, *13*, 3266.
(39) Roy, S. C.; Christensen, P. A.; Hamnett, A.; Thomas, K. M.; Trapp, V. *J. Electrochem. Soc.* **1996**, *143*, 3073.

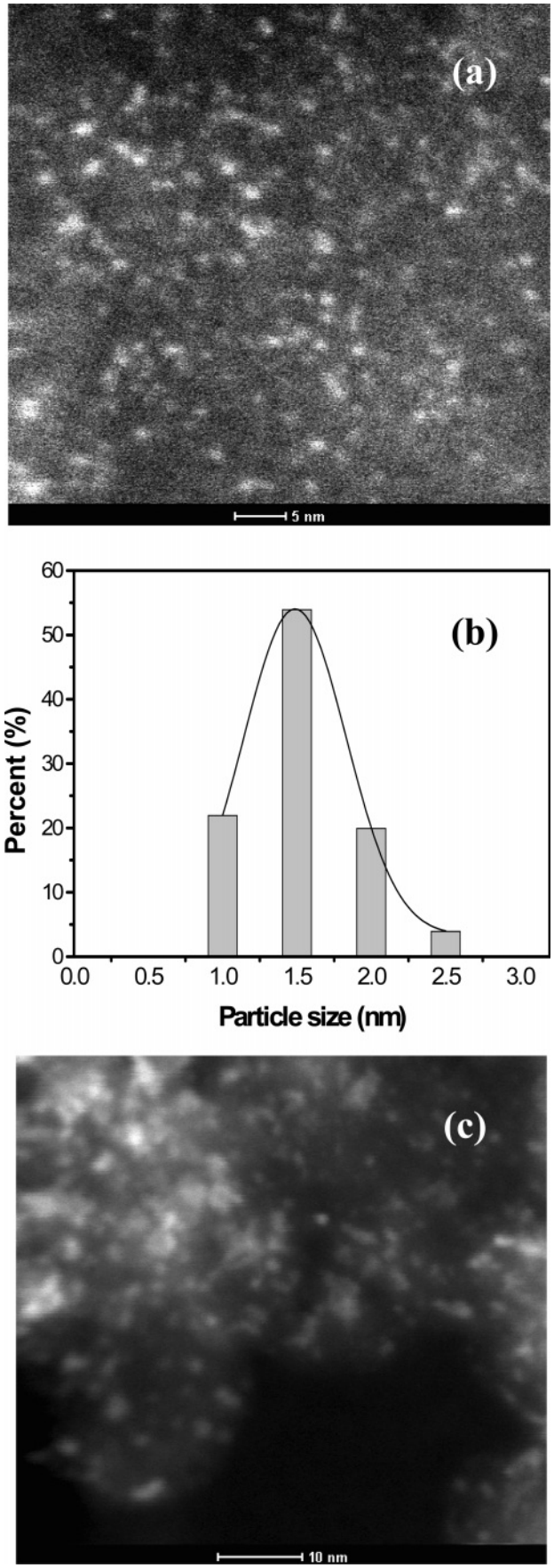

Figure 5. (a) HAADF-STEM micrographs of unsupported metallic tungsten nanoparticles; (b) particle size distribution histogram of tungsten nanoparticles from part a; and (c) HAADF-STEM image of carbon supported tungsten nanoparticles.

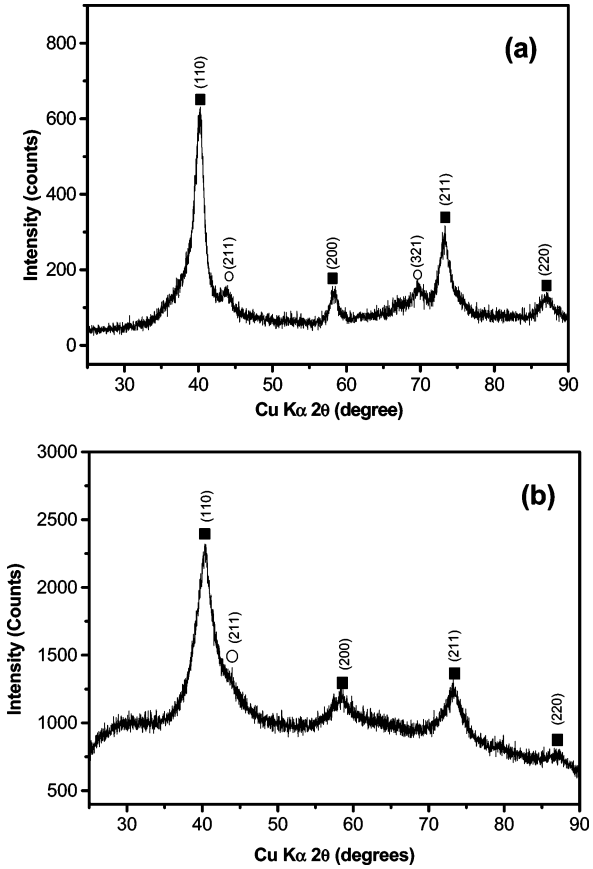

Figure 6. XRD patterns of (a) unsupported and (b) carbon supported metallic tungsten nanoparticles, whereby the symbol ■ represents the α-W phase (PDF number 4-806), and the symbol ○ represents the *β*-W phase (PDF number 47-1319). Samples were prepared using (b) Triton X-100/2-hexanol/cyclohexane/water microemulsion and (a) Brij-30/*n*-heptane/water microemulsion.

support materials to fulfill the needs of various catalysis applications without losing nanoparticle size control.

To verify the formation of tungsten oxide, nanoparticle structures after heat treatments in air at various temperatures were analyzed by XRD as shown in Figure 4. For heat treatment at temperatures lower than 400 °C, only one broad peak was observed in the XRD pattern indicating an amorphous structure. The hydrolysis tungsten product oxidized and crystallized only after heat treating to 400 °C and above as indicated by the defined diffraction peaks. Analysis of the diffraction peaks revealed the presence of hexagonal (symbol "■") and orthorhombic (symbol "○") tungsten oxide (WO_3). The result differs from that previously report[33] where only the monoclinic structure was observed after heat treatment at 500 °C. The crystallization temperature for tungsten oxide formed via hydrolysis is also lower than that reported in the literature.[33] All these differences may relate to the smaller nanoparticles fabricated in this study resulting in higher surface-to-volume ratios and surface energies. The thermodynamics of phase formation and transformation may vary with particle size. Further research is necessary to understand these differences.

3. Synthesis of Metallic Tungsten Nanoparticles. Figure 5a shows the HAADF-STEM image of unsupported metallic

(40) Roy, S. C.; Harding, S. C.; Russell, A. E.; Thomas, K. M. *J. Electrochem. Soc.* **1997**, *144*, 2322.

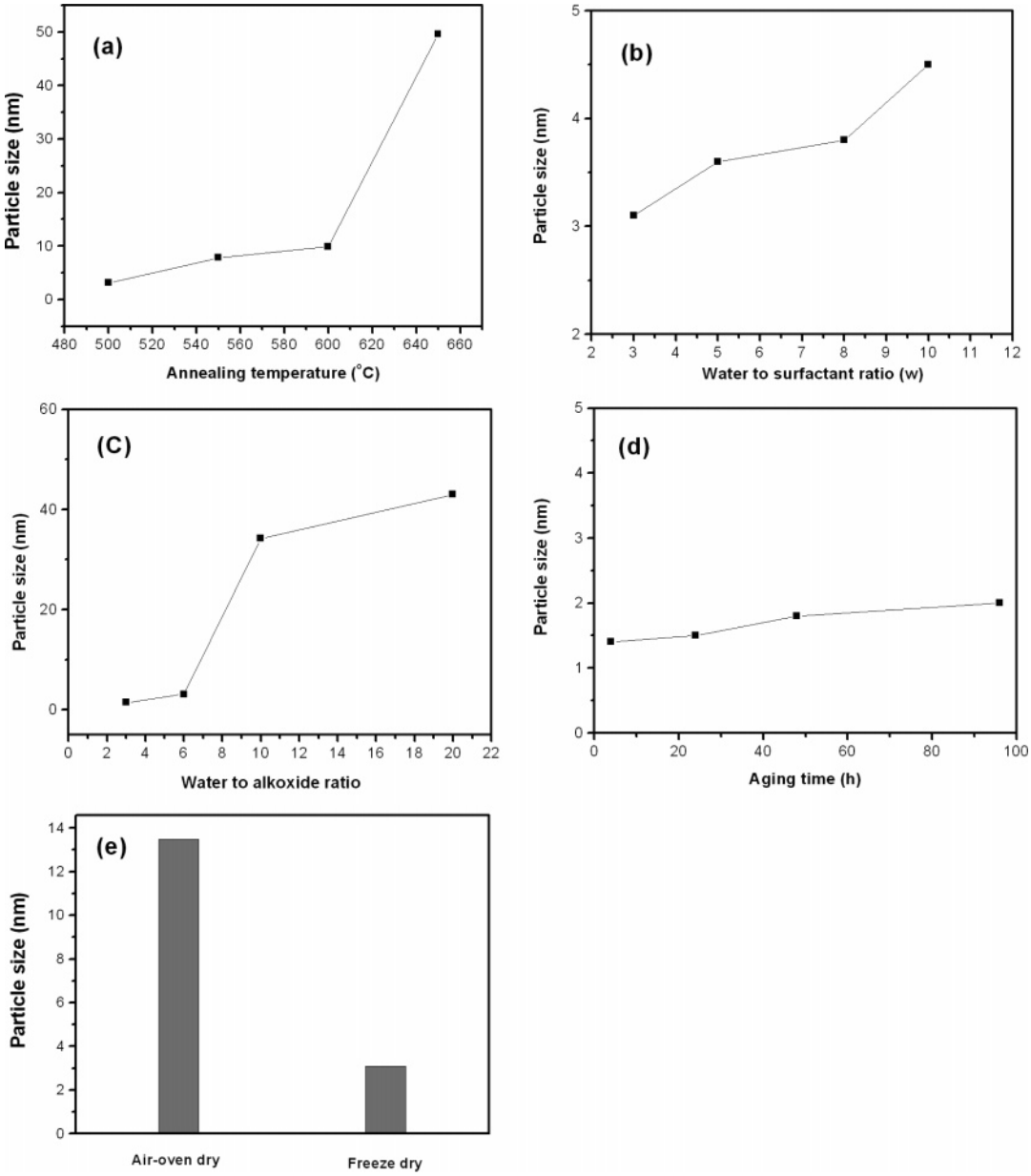

Figure 7. Influence of synthesis parameters, (a) reduction temperature, (b) water-to-surfactant ratio, (c) water-to-alkoxide ratio, (d) aging time, and (e) drying method on the average tungsten nanoparticle size. Synthesis parameters: (a) water/surfactant ratio = 3, water/alkoxide ratio = 6, aging time = 4 h, and freeze drying; (b) water/alkoxide ratio = 6, aging time = 4 h, freeze drying, and heat treated at 500 °C in H_2; (c) water/surfactant ratio = 3, aging time = 4 h, freeze drying, and heat treated at 500 °C in H_2, (d) water/alkoxide ratio = 3, water/surfactant ratio = 3, freeze drying, and heat treated at 500 °C in H_2, and (e) water/surfactant ratio = 3, water/alkoxide ratio = 6, aging time = 4 h, and heat treated at 500 °C in H_2.

tungsten nanoparticles after reduction at 500 °C in H_2. The particles are predominantly spherical with a narrow particle size distribution and an average particle size of 1.5 ± 0.6 nm, obtained from analysis of 200 particles, Figure 5b. In comparison with other synthesis methods, the tungsten nanoparticles fabricated here were small and well-dispersed, whereas the chemical reduction method produced agglomerated amorphous tungsten particles with dimensions of 400−500 nm.[11] Moreover, the well-dispersed nanoparticles reported here offer the capability of being further manipulated in solvent. To the best of our knowledge, this is the first report of synthesized metallic tungsten nanoparticles with such fine particle size and monodispersity.

Figure 5c displays a typical HAADF-STEM micrograph of carbon supported metallic tungsten after heat treatment at 650 °C in H_2. The bright spots are tungsten particles that are well-dispersed on a carbon support with particle size of 1−2 nm. The particle size is also consistent with the crystalline size (1.9 nm) determined from XRD peak broadening. Again, the supported tungsten nanoparticles have sizes similar to those of unsupported nanoparticles indicating that the synthesis does not depend on supporting material properties during preparation.

Figure 6a,b displays the XRD patterns of unsupported and supported metallic tungsten nanoparticles, respectively. The unsupported tungsten nanoparticles have well-defined diffraction peaks at $2\theta = 40.3$, 58.3, 73.2, and 87.0° consistent with body-centered cubic (bcc) α-W and smaller peaks at $2\theta = 44$ and 69.6° consistent with primitive cubic (A15) β-W. Carbon supported tungsten nanoparticles display a similar diffraction pattern with significant peak overlapping. Well-crystallized tungsten nanoparticles can be obtained by

this synthesis method as confirmed by XRD data. The chemical reduction method mentioned above required heat treating temperatures as high as 700 °C to crystallize unsupported tungsten nanoparticles[11] resulting in significant particle growth. As discussed in the surfactant selection section, the selection of surfactants used in this reverse microemulsion synthesis technique does not introduce inorganic impurities as evidenced by EDX analysis (data provided in Supporting Information). In addition, as will be demonstrated later, the phase of metallic tungsten nanoparticles may be controlled by manipulating synthesis conditions.

4. Influence of Synthesis Conditions on Particle Size and Structure. Figure 7a−e illustrates the influence of synthesis conditions on the size of unsupported metallic tungsten nanoparticles. By manipulating these synthesis parameters, tungsten nanoparticles with various particle sizes can be fabricated.

The effect of heat treatment temperature on tungsten particle size is shown in Figure 7a. The average particle size increases slightly with temperature from 500 °C to 600 °C. However, above 600 °C the particles grow rapidly. The results indicate that appropriate reduction temperatures are very important in controlling the tungsten nanoparticle size: a too low heat treatment temperature may not be sufficient to reduce the tungsten hydrolysis products to the metallic state, but a too high reduction temperature will cause the particles to grow too rapidly. In conventional synthesis, temperatures as high as 1000 °C were needed to reduce the tungsten oxide nanoparticles to the metallic state.[6] The significantly lower reduction temperature in this report (500 °C) results from two possible reasons. Again, one is the size effect of the nanoparticles fabricated by the reverse microemulsion method being much smaller. Another is the hydrolysis products, likely hydrated tungsten dioxide or tungsten hydroxide, that may be more easily reduced than tungsten oxide.

Figure 7b displays the effect of water-to-surfactant ratio on tungsten particle size. As discussed previously, the particle size of tungsten increases with increasing water-to-surfactant ratios. The size and morphology of the hydrolysis products influence the final size of metallic tungsten. The smaller sized hydrolysis products generally lead to smaller tungsten nanoparticles; however, agglomeration of small sized hydrolysis products may form large particles after heat treatment.[41] Ratios of water to surfactant greater than 10 were not studied. High water-to-surfactant ratios may lead to increased particle size and size polydispersity and can create unstable microemulsions resulting in much larger tungsten particles, counter to the purpose of this study.

The effect of the water-to-alkoxide ratio on the size of tungsten nanoparticles is plotted in Figure 7c. The ratio of water to alkoxide has pronounced influence on the particle size of tungsten. Very large particles were formed when the ratio of water to alkoxide exceeds ~ 6. Synthesis with high water-to-alkoxide ratios (>10) resulted in hydrolysis products that were very difficult to precipitate (even after an extended time) indicating that the particles formed were either very small and discrete or aggregated into very low density agglomerates. Generally, hydrolysis reactions favor high water-to-alkoxide ratios whereas condensation processes favor low water-to-alkoxide ratios. The high water-to-tungsten alkoxide ratios used in the aforementioned syntheses led to hydrolysis rates that exceeded condensation rates, thus resulting in highly porous agglomerates. Adjacent agglomerates tend to aggregate, forming larger particles after heat treatment as reported before.[41]

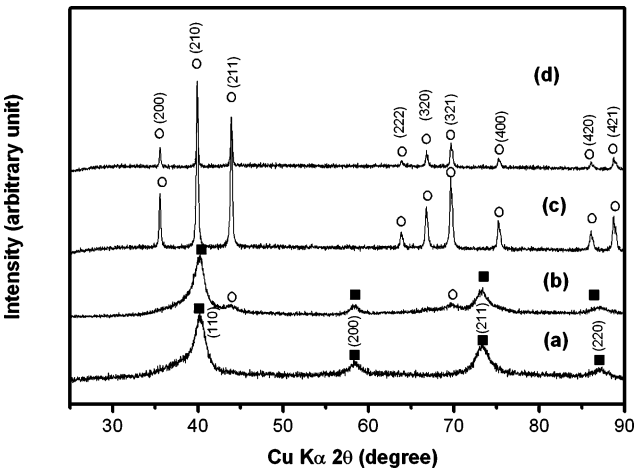

Figure 8. XRD patterns of tungsten nanoparticles prepared with water-to-alkoxide ratios of (a) 3, (b) 6, (c) 10, and (d) 20, whereby the symbol ■ represents the α-W phase (PDF number 4-806) and the symbol ○ represents the β-W phase (PDF number 47-1319).

Figure 7d illustrates the effect of aging time on the size of tungsten nanoparticles. The average particle size increases gradually with aging time. Appropriate aging time is required to ensure that the hydrolysis reaction and the condensation of hydroxyl species are completed. Within the time range studied, aging time was not a critical parameter in controlling tungsten particle size.

The effect of the drying method on tungsten particle size is displayed in Figure 7e. The particles collected from the freeze-drying method were significantly smaller than those from the air-oven drying. Unlike air oven drying, freeze drying tends to keep the original structure of nanoparticles after hydrolysis and condensation. Additionally, the particles collected from freeze drying exhibit higher tolerance against agglomeration at high temperatures.

Besides controlling the particle size, the ability to control the structure of tungsten nanoparticles may be of interest for certain applications. Metallic tungsten has two different structures: α-W with a bcc structure and β-W with a cubic (A15) structure. Each structure displays unique physical properties such as conductivity, superconducting transition temperature, and so forth.[42] An interesting observation in this study was that by manipulating synthesis conditions, the tungsten nanoparticle with different structures could be prepared. Examples are shown in Figure 8, where pure α-W nanoparticles were prepared in a water-to-alkoxide ratio of 3 (scan a); mixed α-W and β-W nanoparticles were obtained by increasing the water-to-alkoxide ratio to 6 (scan b); and

(41) Zarur, A. J.; Hwu, H. H.; Ying, J. Y. *Langmuir* **2000**, *16*, 3042.

(42) Gibson, J. W.; Hein, R. A. *Phys. Rev. Lett.* **1964**, *12*, 688.

pure β-phase tungsten nanoparticles were fabricated by further increasing the water-to-alkoxide ratio to 10 or 20 (scans c and d). Phase transformations in the tungsten thin film has been reported in the literature.[43,44] The metastable β-W phase transforms to the α-W phase by increasing temperature, film thickness, and changes of oxygen partial pressure. The phase transformation may even occur at room temperature and is enhanced by low-temperature heat treatments (150−200 °C).[45] In addition, the formation of β-W can be stabilized by oxygen contamination in the film.[43] Unlike these findings, the β-W nanoparticles fabricated in this study do not transfer to the more stable α-W even after heat treating at 500 °C. Presently, it is not clear why the β-phase tungsten prepared by our method is so stable and how the water-to-alkoxide ratio influences the structure of the tungsten nanoparticles. Additional study is necessary to fully understand the phenomena.

(43) Rossnagel, S. M.; Noyan, I. C.; Cabral, C. J. *J. Vac. Sci. Technol., B* **2002**, *20*, 2047.
(44) Weerasekara, I. A.; Shah, S. I., Baxter, D. V.; Unruh, K. M. *Appl. Phys. Lett*. **1994**, *64*, 3231.
(45) Petroff, P.; Sheng, T. T.; Sinha, A. K.; Rozgonyi, G. A.; Alexander, F. B. *J. Appl. Phys.* **1973**, *44*, 2545.

Conclusions

A reverse microemulsion-mediated synthesis protocol has been demonstrated to prepare nanosized, unsupported, and supported metallic tungsten and tungsten oxide particles of less than 5 nm. By manipulating synthesis conditions, such as water-to-surfactant ratio, reduction temperature, water-to-alkoxide ratio, and drying methods, the size and structure of metallic tungsten nanoparticles can be controlled. The ultrafine powders of metallic tungsten and tungsten oxides prepared by the reverse microemulsion method may find wide applications in various fields such as catalysis, electronics, illumination, gas sensors, and so forth.

Acknowledgment. The authors acknowledge Eric Kreidler for kind assistance in preparing the manuscript.

Supporting Information Available: TGA-DSC analysis of surfactants, EDX analysis of tungsten oxide and metallic tungsten, and low-magnification TEM micrographs (PDF). This material is available free of charge via the Internet at http://pubs.acs.org.

CM052320T